Non-covalent close contacts in fluorinated thiophene-phenylene-thiophene conjugated units: understanding the nature and dominance of O···H versus S···F and O···F interactions towards the control of polymer conformation

Tetiana Kharandiuk,[†] Eman J. Hussien,[‡] Joseph Cameron,[‡] Romana Petrina, [†] Neil J. Findlay,[‡] Roman Naumov,[§] Wim T. Klooster,[∫] Simon J. Coles,[∫] Qianxiang Ai,[#] Stephen Goodlett,[#] Chad Risko*,[#] and Peter J. Skabara*,[‡]

AUTHOR ADDRESS.

[†]Department of Technology of Organic Products, Lviv Polytechnic National University, Lviv, Ukraine

[‡]WestCHEM, School of Chemistry, University of Glasgow, Glasgow G12 8QQ, UK

[§]Institute for Problems of Chemical Physics of Russian Academy of Sciences, Chenogolovka, Russia

[∫]School of Chemistry, University of Southampton, Southampton, SO17 1BJ, UK

[#]Department of Chemistry & Center for Applied Energy Research (CAER), University of Kentucky, Lexington, Kentucky 40506 USA

ABSTRACT: Using a simple π-conjugated trimer, EDOT-phenylene-EDOT (where EDOT = 3,4-ethylenedioxythiophene), we evaluate the effect that fluorine substituents have upon changes in conformation, conjugation and oxidation potentials in π-conjugated structures. These variations are assessed as a function of the fluorine atom's propensity to feature in hydrogen and/or halogen bonding with other heteroatoms. The molecular motif was chosen because the EDOT unit presents the possibility of competing O···X or S···X non-covalent contacts (where X = H or F). Such non-bonding interactions are acknowledged to be highly influential in dictating molecular and polymer morphology and inducing changes in certain physical properties. We studied four compounds, beginning with an unsubstituted bridging phenylene ring and then adding one, two, or four fluorine units to the parent molecule. Our studies involve single crystal XRD studies, cyclic voltammetry, absorption spectroscopy and density functional theory calculations to identify the dominant non-covalent interactions and elucidate their effects on the molecules described. Experimental studies have also been carried out on the corresponding electrochemically synthesized polymers to confirm that these non-covalent interactions and their effects persist in polymers. Our findings show that hydrogen bonding and halogen bonding feature in these molecules and their corresponding polymers.

Introduction

The use of fluorine as a substituent in organic semiconductor materials can lead to significant enhancement in device performance for organic solar cells and field effect transistors. One of the main reported reasons, in addition to the strong electron-withdrawing nature of fluorine atoms, is due to the interactions that fluorine can have with a neighboring intramolecular hydrogen[1] and other atoms that lead to weak but persistent heteroatom interactions.[2-3] These associations, categorized as either hydrogen bonding or halogen bonding,[4-5] can give rise to planar and rigid architectures within a π-conjugated unit, which in turn can strongly support π-π interactions between molecules or polymer chains. By increasing the dimensionality of orbital overlap, from single conjugated chains to the bulk, charge transport is enhanced throughout the semiconductor material.[6] Fluorine-heteroatom interactions are driven by hydrogen bonding and other types of non-covalent connections, such as electrostatic and three-center two-electron bonds.[7] In a complex structure, as is often seen in organic semiconductor molecules and polymers, there are several potential combinations of heteroatoms that could define the overall low energy conformation. Understanding the nature and strengths of these interactions is therefore important in the design of new structures where the conformation of the molecule/polymer can play an important role in the key physical properties of the organic semiconductor.

In our previous work, we studied chalcogen-chalcogen and chalcogen-pnictogen intramolecular and intermolec-

ular non-covalent contacts and their effects on polymer conformation and molecular self-assembly.[2] Even in relatively simple structures, the conformations resulting from such interactions can be difficult to predict. For example, compounds **1**[8] and **2**[9] in Chart 1 have terthiophene units that are held in planarity through close contacts between the sulfur atoms of the peripheral thiophenes and the two sulfur substituents of the central thiophene, as shown. However, in compounds **3**-**5**,[3, 10] the molecules are quite twisted and there seems to be competition between S···O

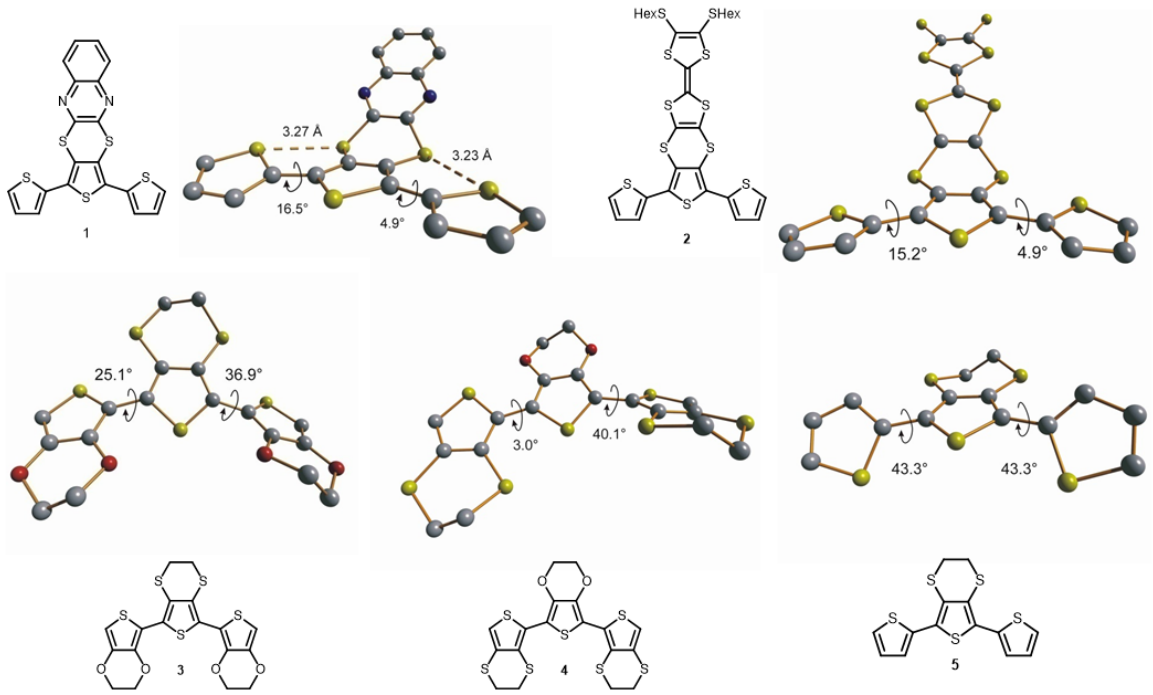

Chart 1

and S···S interactions. From a comparison of the polymers PEDOT and PEDTT (Chart 2), we observe that S···O interactions are highly attractive and S···S strongly repulsive, leading to the large difference in the optical band gaps of these polymers due to the high co-planarity between EDOTs and the highly twisted nature of the PEDTT structure.[3] Such subtle differences in the chalcogen atom can result in an even larger shift of the band gap – a variation of *ca*. 1 eV was observed between polymers **6** and **7** (Scheme 2),[11] due to the highly twisted nature of the bis-EDTT units within the polymer structure.

The role of the fluorine atom in organic semiconductors has become a highly topical discussion point. It can have a beneficial effect as a simple substituent, for example by tuning the energy levels of donor and acceptor materials towards higher efficiency organic solar cells.[12] However, the main interest in fluorine in π-conjugated materials has centered on its ability to provide conformationally locked structures for band gap tuning and good charge transport properties. The most common examples of fluorine-substituted materials are found in copolymers of thiophene and 2,1,3-benzothiadiazole,[13-15] and in structures that incorporate fluorinated phenylene units.[16-27] With the above in mind, our intention in this work was to probe further into the role of the fluorine atom as an influential substituent in the control of conformation in π-conjugated structures, focusing on the nature of the intramolecular interactions and the competition between hydrogen bonding and chalcogen-fluorine bonding.[28-31]

Results and Discussion

Crystallography. Whilst heteroatom interactions are important,[2, 7] hydrogen bonding within conjugated polymers can be stronger. In this paper, we focused our study on fluorinated phenylene linkers between EDOT units to evaluate the potential non-covalent interactions in structures based on this motif (**0F**-**4F**, Chart 3). The possible interactions in these molecules are: S···F, O···F, O···H and S···H. Sotzing *et al*.[32] published the single crystal X-ray structure of compound **0F** and found the torsion angles between the thiophenes and the benzene ring to be 27.5(2)°, a value that does not support the presence of hydrogen bonding between the phenylene ring and the chalcogen atoms.

The structures of **1F**-**4F** are shown in Figure 1; the synthesis of compounds **1F** and **2F** have been reported previously,[33-34] but their molecular structures have not been studied until this work. The immediate observation in these structures is the difference between the molecular conformations of **2F** and **4F**. Compound **4F** is significantly twisted with a torsion angle of 135.7°, whereas **2F** is planar with a torsion angle of 178.2°. There are only two possible non-covalent interactions in **4F**, *viz*. S···F and O···F contacts. Since oxygen and fluorine are too electronegative to form a non-covalent bond, one can conclude that the

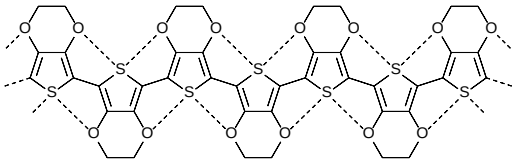

PEDOT
Eg = 1.63 eV

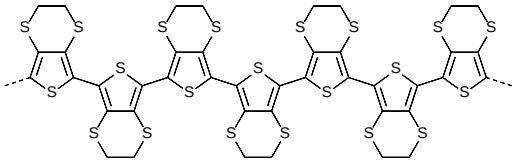

PEDTT
Eg = 2.15 eV

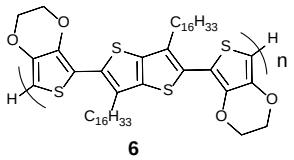

Eg = 1.53 eV

6

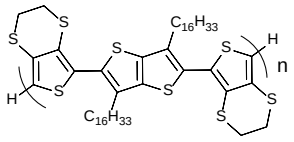

Eg = 2.49 eV

7

Chart 2

repulsive O···F interaction is stronger than the S···F attractive interaction. Comparing **4F** with the analogous compound **8**[16] (Chart 4), the maximum torsion angle across the entire molecule is 4.08°, so one can see that S···F can be associated with a planar geometry. However, the structure of molecule **9**[17] is also highly planar (1.18° torsion angle between rings), and clearly shows that F···H pairing is preferred over S···F, indicating that in compound **8** planarization could be due mainly from hydrogen bonding. As structure **8** has two possible connections, **2F** also has a choice of non-covalent interactions, namely S···F, S···O and O···H. The high electronegative pairing of S···O is avoided and there are close S···F contacts and an O···H hydrogen bond.

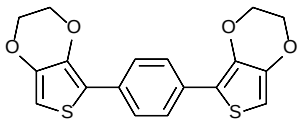

0F

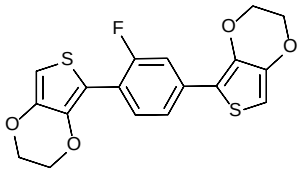

1F

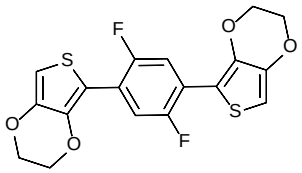

2F

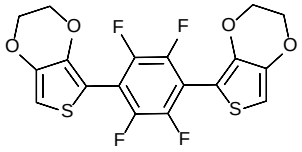

4F

Chart 3

In the crystal of **1F**, the molecule is frustrated and there is disorder in the phenylene ring with the fluorine atom occupying two positions. Again, the O···F associations are avoided and there are close contacts between S···F and O···H atoms. The disorder arises from weaker non-covalent bonds (*vide infra*), with longer contacts than those seen in **2F** and consequently a significant increase in the torsion angle.

From the crystallographic studies of **0F**-**4F**, **8** and **9**, we conclude: (i) hydrogen bonding and S···F interactions can coexist to give planar structures; (ii) O···F repulsion is strong and is avoided in molecules **1F**-**4F**; (iii) O···H hydrogen bonding is not observed in the twisted structure of **0F**, indicating that the fluorine substituents in **1F** and **2F** are important in increasing the positive nature of the phenylene hydrogen atoms to promote hydrogen bonding with an EDOT oxygen atom; (iv) determining the relative importance of S···F and O···H non-covalent bonds is inconclusive from crystallographic studies, so a computational approach is required to elucidate the matter (*vide infra*). However, since crystal packing forces can also be influential in shaping the conformation of the molecules studied, we performed solution state absorption spectroscopy and cyclic voltammetry experiments to determine whether or not the conformers detailed above persist in solution.

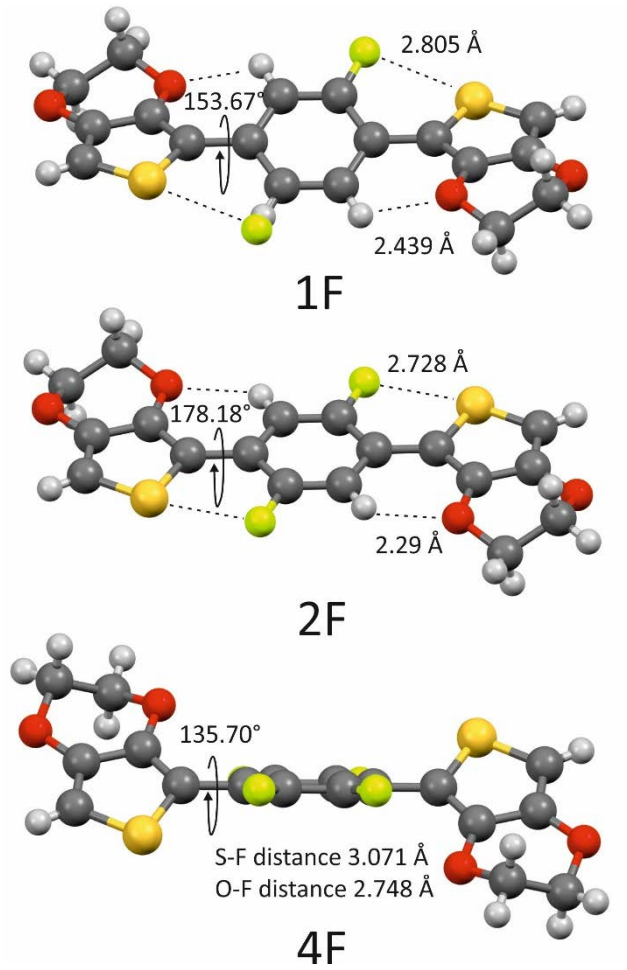

Figure 1. Molecular structures of compounds **1F**, **2F** and **4F**, determined by single crystal X-ray diffraction studies. Torsion angles are measured across the four carbon atoms between each aromatic units. (sum of the van der Waals radii: H + F = 2.67 Å, S + F = 3.27 Å, O + F = 2.99 Å).

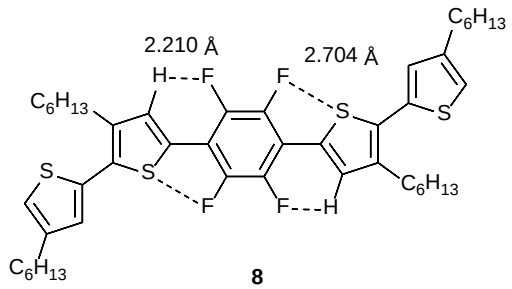

8

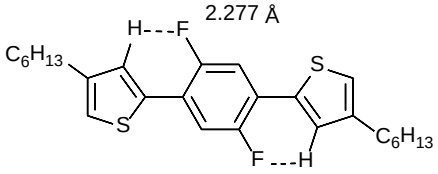

9

Chart 4

Absorption Spectroscopy. In this section we aim to corroborate the solid-state crystallographic studies with solution absorption spectroscopy, primarily to provide evidence that the conformers that are observed in the solid state exist in solution. The electronic absorption spectra in dichloromethane for compounds **1F**-**4F** are shown in Figure 2 and the full set of absorption spectroscopy data is given in Table S1 (SI section). The spectra for **1F** and **2F** have fine structure, which is an indication of a rigid and persistent conformation in solution. Compound **1F** and **2F** have four sets of peaks, with the largest centred at 343 nm and 346 nm, respectively. On the other hand, compound **4F** has a broad absorption band with a maximum at 309 nm. The highly twisted nature of compound **4F** is therefore present in the solution state and the higher energy absorption maximum, compared to **1F** and **2F**, shows a significant loss in conjugation due to the distorted structure. The minor difference in the absorption maxima between **1F** and **2F** could be due to either greater planarity in **2F**, as seen in the crystal structure, or a substituent effect of the additional fluorine atom. To probe this in greater detail, cyclic voltammetry experiments were performed on the three materials.

Cyclic Voltammetry Experiments. Cyclic voltammetry (CV) measurements were conducted using a small amount of ferrocene as an internal standard. This experiment was repeated three times for reproducibility. A gold disk working electrode was used for these experiments with applied iR compensation test at a sensitivity of 10^{-4} A/V. The CVs of compounds **1F**-**4F** are shown in Figure 3. All materials display a single irreversible oxidation process. Compound **2F** has an E_{ox} of 0.70 V, whereas that of **1F** is lower at 0.58 V. Assuming that the site of oxidation is the EDOT unit, this difference can be attributed to the higher loading of fluorine atoms in **2F**, which has a stronger electron withdrawing effect on the EDOT substituent and therefore raises its oxidation potential accordingly, with respect to **1F**. However, this explanation does not befit the electrochemical behavior of **4F**, since one would expect the same rationale to predict an even higher oxidation potential due to the presence of four fluorine atoms. Indeed, the oxidation potential is far lower for **4F** at 0.42 V and this can be explained by the twisted nature of the molecule in solution state. Since there is no conjugation between the aromatic units, nor any short heteroatom contacts in this molecule, the EDOT units can be regarded as being unaffected by the fluorine atoms and therefore there is a much-reduced electron withdrawing effect to raise the oxidation potential of **4F**.

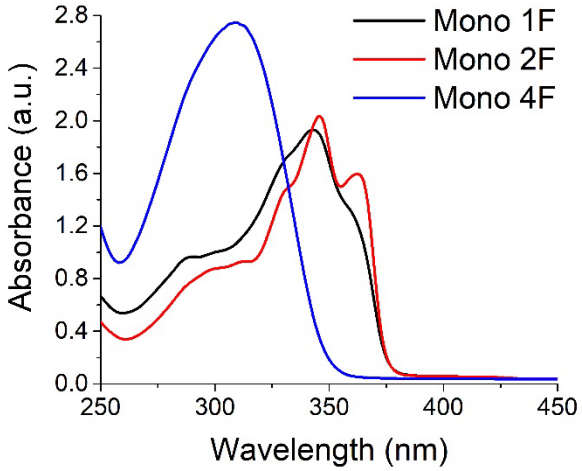

Figure 2. Absorption spectra for compounds **1F**-**4F** in dichloromethane solution.

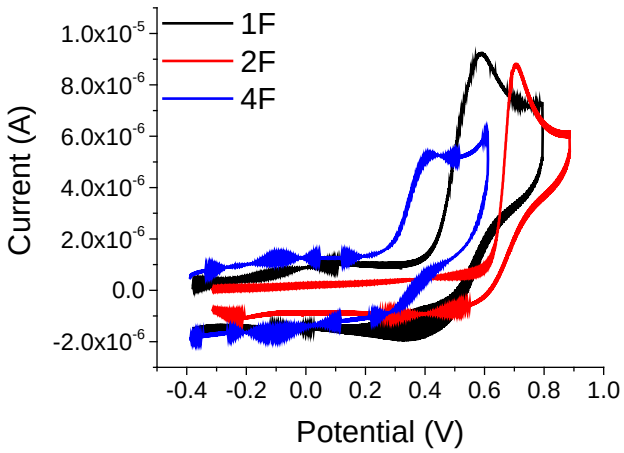

Figure 3. Cyclic voltammograms for compounds **1F**-**4F** in dichloromethane solution.

So far, the absorption spectroscopy and CV data show that the conformations observed in the crystalline solid state persist in solution state. Whilst these studies were based on simple molecules, it was interesting to investigate whether such conformers exist in polymer structures based on **1F**-**4F**. The monomers were electropolymerized with 80 multisweep segments over a potential range that covered the oxidation wave of the monomers. The experiments were performed first on the button of a gold disk working electrode and then repeated using indium tin oxide (ITO) glass transparent electrode using the same conditions. The CVs depicting the growth of the polymers are given in Figure S1.

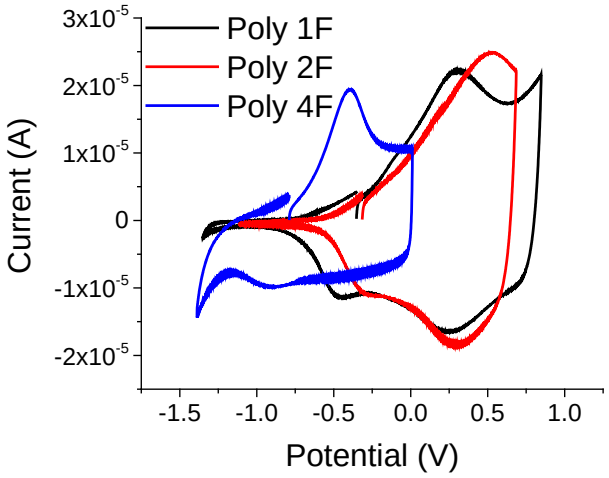

Figure 4. Cyclic voltammograms for the electrogenerated polymers of **1F**-**4F** in dichloromethane solution.

The cyclic voltammograms for the polymers (Figure 4), were measured in a monomer free solution using a Au electrode for the CV data and an ITO working electrode for subsequent absorption spectroscopy measurements. After the growth cycles, the polymers were dedoped by cycling in a region of redox inactivity (this is typically performed between the oxidation and reduction processes), for around three hours in a monomer free solution. The trend in oxidation potentials follow the pattern observed in the monomer CVs. The oxidation peak for poly(**1F**) is 0.32 V and for poly(**2F**) this value is raised to 0.50 V which, as expected, are both lower than the oxidation potentials of the respective monomers. For poly(**4F**), the oxidation potential is -0.39 V, which is significantly lower than the value for the monomer (0.42 V). It can be assumed that the shift in the oxidation potential is due to the presence of the bis-EDOT unit within the polymer structure, which is known to be highly planar[35] and more electroactive than the single EDOT molecule. Again we postulate that the tetrafluorophenylene units remain highly twisted in the polymer, since this would shift the oxidation potential of the polymer to higher values if this was not the case. To probe this assumption further, absorption spectroscopy was performed on the as-grown and dedoped films of the polymers.

Compared to the monomers **1F** and **2F**, a large bathochromic shift of the absorption maxima was observed for poly(**1F**) and poly(**2F**) (λ_{max} at 499 nm and 503 nm, respectively). This shift is attributed to the higher conjugation length in the conjugated polymer structures. Our results show no detectable absorption for poly(**4F**)on ITO glass. Bearing in mind the absorption maximum of **4F** (309 nm), a similar magnitude of shift should be expected for a planar polymer and this should be observable at λ_{max} > 400 nm. From the hypothesis above, in which the tetrafluorophenylene unit is twisted and disrupts conjugation through the chain, the absorption signature of bis-EDOT should be observed. However, the absorption spectrum of bis-EDOT (Figure S2) shows that there are no significant features above 350 nm, which is the cut-off point for ITO

glass in absorption spectroscopy measurements. This observation lends further proof of the highly twisted nature of poly(**4F**) and we can conclude that the conformers observed in the crystalline solid state persist in solution and in the repeat units of the polymer structures.

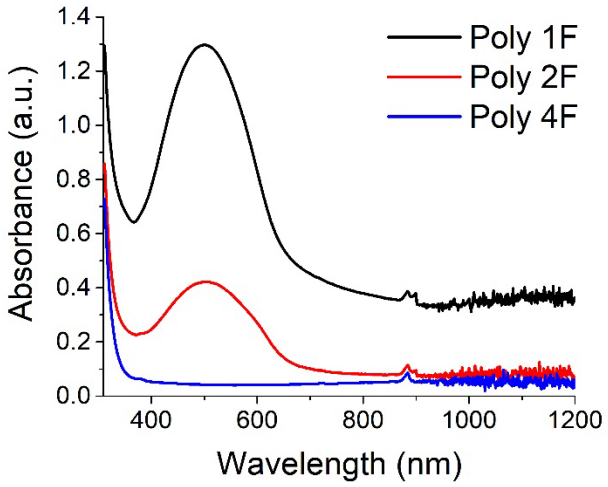

Figure 5. Solid state absorption spectra on ITO glass of polymers derived from **1F**-**4F**.

The emission spectra of compounds **1F**, **2F** and **4F** were recorded in dichloromethane solution and are shown in Figure S3. Similar to the absorption spectra, the emission profiles of **1F** and **2F** show fine structure and are almost identical. The main peak values for **1F** (**2F**) are 379 nm (375 nm) and 395 nm (394 nm), with a shoulder at 416 nm (416 nm). The spectrum for **4F** is broad and ill-defined in comparison and this provides further evidence of more persistent conformers for **1F** and **2F** in solution. Interestingly, the photoluminescence quantum yields for **1F** and **2F** in solution were 19.3% and 12.6%, respectively, whereas the value for **4F** could not be measured because of its weak emission.

Density functional theory (DFT) investigation. With a robust set of experimental data pointing to strong variations in the structural, redox, and optical characteristics of **1F**-**4F** as a function of fluorination, we aimed to dig deeper into the nature of the intramolecular interactions driving these differences. All isolated molecule DFT calculations were carried out at the ωB97XD/jun-cc-pvdz level of theory. In addition to **1F**-**4F**, we also broke the molecules down into two moiety constructs (one EDOT plus the phenyl group) to further isolate the nature of the intramolecular interactions (Figure 6); we note that the fluorine positions are labeled in Figure 6 for future reference. To evaluate the impact of fluorine substitution on the molecular conformation, it is illustrative to examine the potential energy surface (PES) as a function of the dihedral angles among the aromatic units; here, the PES scans were performed by twisting EDOT around the bond between EDOT and the phenyl ring.

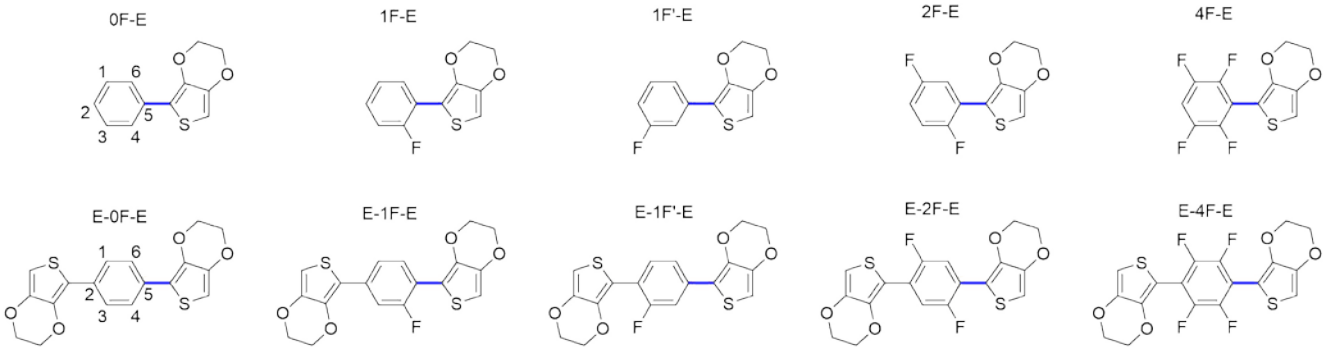

Figure 6. Two- and three-moiety structures used in the DFT investigation. The bond related to PES scan is denoted by the blue color.

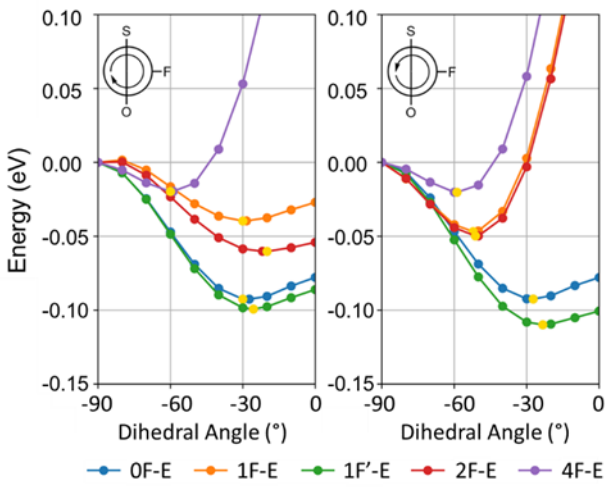

Figure 7. PES for the dihedral angle between the aromatic units in the two-moiety structures, where the dihedral angle between the EDOT and phenyl ring is twisted from -90° to 0°. The two subplots represent different twist directions, as shown in the inset schemes, where F represents the fluorine (if any) that is in close proximity to the EDOT unit.

We start with the two-moiety structures, referred to as EDOTB, and their PES (Figure 7), where two half-scans are performed for each structure based on twisting direction; the yellow dots in the figure represent the minimum position for each half-PES scan. Notably, there is a rapid rise in the PES for 1F-E, 2F-E in the second half-scan, and 4F-E in both half-scans that can be directly attributed to repulsive O···F interactions. In general, fluorine substitution at positions labeled 4 or 6 on the phenyl ring reduces the rigidity of the dihedral torsion. Interestingly, the local minimum in the first half-scan of 1F-E is less stable than that in the second half-scan, where no direct S···F interaction can be established. Hence, instead of acting as an agent to "lock" the structure into a quasi-planar configuration, such substitution tends to reduce the transition barrier among the local minima on the PES.

Analyses of the non-covalent interactions based on the atoms-in-molecules (AIM) approach confirms the existence of S···F bond critical points (BCP) at the scan minima of 1F-E and 2F-E (selected AIM parameters are presented in Table S2). The S···F distances in these situations are smaller than the sum of their van der Waals radii (3.27 Å). The nature of these interactions is revealed by reduced density gradient (RDG) analyses (Figure 8), where both weak attractive and repulsive interactions are identified by the sign of λ_2, the second large eigenvalue of electron density Hessian matrix.[36] The existence of such repulsive interactions, indicative of oft-referred steric effects, is in agreement with the (3, +1) type BCP found at the center of C-C-C-F...S ring. While previous studies have discovered S···F interactions as halogen-type bonds,[37-39] we note that in these EDOTB structures that the S···F interaction is limited and the charge depleted region around sulfur does not point towards fluorine, as illustrated by the electron density Laplacian (Figure 9).

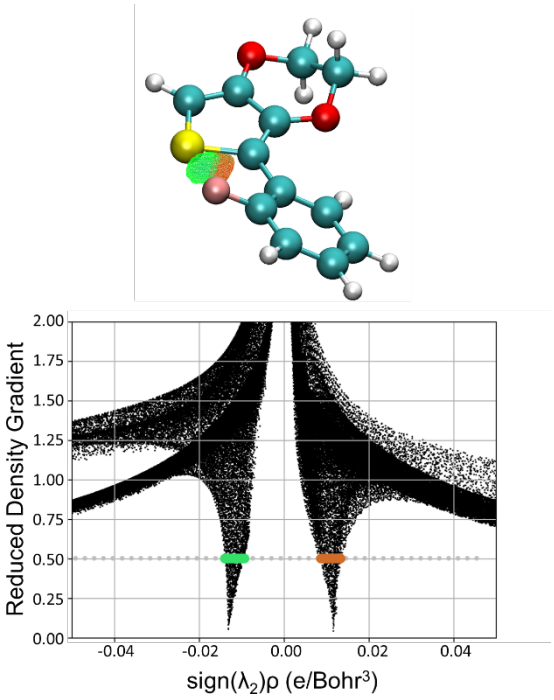

Figure 8. Top: RDG isosurface with RDG=0.5 that is colored based on the sign of λ_2 as shown in the scatter plot. Bottom: Scatter plot of the RDG values for the S···F interaction versus sign(λ_2)ρ, where λ_2 is the second large eigenvalue of electron density (ρ) Hessian matrix. The data is collected in a 3 Å × 3 Å × 3 Å box evenly sampled with 216,000 grid points. The horizontal line represents the isovalue that is shown in the RDG isosurface on the right.

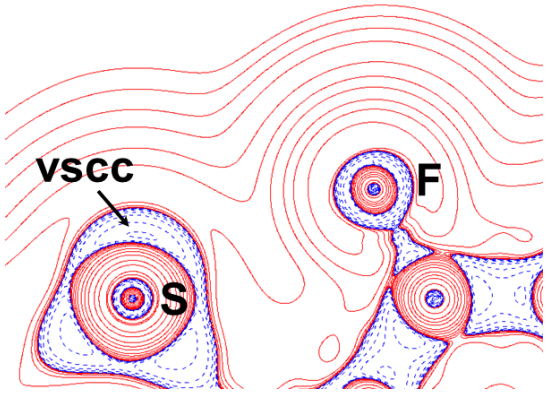

Figure 9. Contour map of electron density Laplacian in the S···F region. Contour lines are colored red and blue for negative and positive values, respectively. The charge depletion region on sulfur is labeled (valence shell of charge concentration, *vscc*).

On the other hand, fluorine atoms substituted at positions labeled 1 or 3 on the phenyl ring result in more rigid structures. Here, it is apparent, however, that it is the O···H interaction that gains prevalence. The strength of

this interaction is significantly affected by the bond acidity of the C-H bond, as the electronic density at the BCP increases significantly after fluorine atoms are introduced onto the phenyl ring. By defining V_H as the electrostatic potential at H without the contribution from the H nucleus itself, we can evaluate the pKa of C-H bond, which is inversely correlated with $|V_H|$.[40] Interestingly, while generally a larger C-H bond acidity yields a stronger O···H interaction, E-1F seems to be an outlier with a larger $|V_H|$ but also a stronger O···H interaction comparing to E-1F' (2nd). This could be addressed by steric effects due to S···F interactions in E-1F that partially bend the structure, leading to a closer O···H pair (Figure 10). Here, one can surmise that the relative structural rigidity of the two-moiety structures comes from strong O···H interactions, and not necessarily from the S···F interactions.

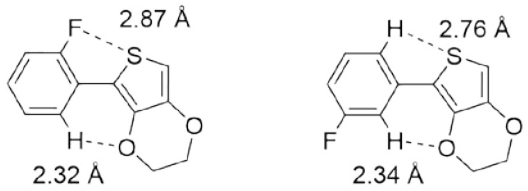

Figure 10. Structural features in the optimized structures of E-1F (left) and E-1F' in the second half-scan (right).

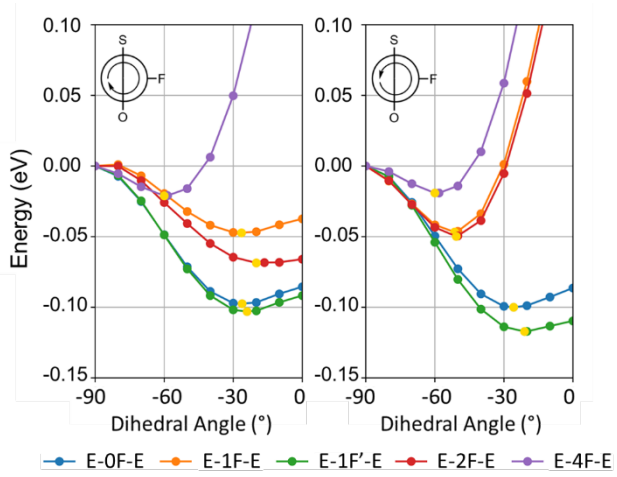

Figure 11. PES scans of the three-unit structures where the dihedral angle between EDOT and phenyl ring is twisted from -90 to 0. The two subplots represent different twist directions, as shown in the inset schemes, where F represents the fluorine (if any) that is in close proximity to the EDOT unit.

Figure 11 presents the full molecule, three-moiety PES, which are quite similar to those of the fluorinated EDOTB. The effect of fluorine substitution is highlighted by the optimized geometry of E-1F-E (which is identical to E-1F'-E), where the dihedral angle between EDOTB and EDOT is more twisted with fluorine at the 4 or 6 position of the phenyl ring.

The structural tendencies described for the isolated molecule structures are, indeed, less transparent in the solid state, which is a function of the significant disorder identified in the crystal structures, in particular for **1F**. As there are four molecules per unit cell and two disorder groups per molecule in **1F**, $2^4 = 16$ configurations could be present in the crystal (assuming that the periodicity remains). Periodic DFT calculations were carried out to determine the cohesive energies of these 16 configurations (Table S2). Notably, the cohesive energies across all molecular configurations are very similar. Further, analyses of the inter-moiety dihedral angles of the most stable packing configuration (Table S3) show (albeit modest) variation in the same dihedral angles among the four molecules that comprise the unit cell. These results, along with various intermolecular short contacts (note that cifs are available in the SI for the 16 configurations considered), suggest that direct evaluation of intramolecular S···F interactions can be a difficult task, and that the role of the S···F interaction may not always be clearly defined.

Conclusions

The molecular structures under investigation demonstrate the complexity of potential interactions available within π-conjugated molecules that contain fluorine. From our joint experimental and theoretical studies it can be concluded that hydrogen bonding is the dominant interaction that defines the conformation in compounds **oF-4F**. In this series, the preferred conformers are facilitated only in part by weak S···F halogen bonds, even to the extent that steric interactions bend the molecule and push H/F substituents closer together. Hydrogen bonding is further facilitated by the increased acidity of the Hs on the phenylene ring, due to the presence of fluorine at adjacent positions; note that the structure of **oF** is highly twisted because of the absence of fluorine in that compound and the subsequent reduction in H-bonding strength. Finally, the strong repulsive nature of the O···F interaction leads to the highly twisted conformer observed in **4F**. This repulsive interaction is far stronger than the weak attraction between sulfur and fluorine atoms. The preferred conformations of the molecular structures are persistent in solution and also in polymers. This is an important insight for the design of monomers towards targeted properties, such as HOMO/LUMO energy levels and electronic band gaps. In particular, adopting a twist unit into a polymer structure can retain the electronic properties observed in the monomer.

Materials and Methods

Compound **oF** was synthesized according to the literature.[32] The synthesis of compounds **1F-4F** and their characterisation data are given in the Supporting Information section.

Cyclic Voltammetry. Measurements were performed on a CH Instruments 660E Electrochemical workstation at a scan rate of 0.1 V/s. Blank cell was performed as an initial and a final cleaning step before measuring. Three electrodes were used in these experiments: gold (Au) disk as a working electrode, platinum (Pt) wire as a counter electrode, silver (Ag) wire as a reference electrode. Tet-

rabutylammonium hexafluorophosphate ($TBAPF_6$) (Sigma Aldrich) was used as the electrolyte (0.1 M) in dry dichloromethane (DCM). The substrate concentration was 0.1 mM. Solvents were obtained from an in-house solvent purification system. All glassware was cleaned, rinsed with DCM and dried at 120 °C in an oven overnight prior to use. Each value was corrected to the redox potential of ferrocene.

UV-Vis-NIR Spectroscopy: UV/Vis spectra were recorded using a Shimadzu UV-2600 Spectrophotometer in the range 200-1200 nm, using a 1 cm path length quartz cell.

Computational Methods:

Density functional theory (DFT) calculations were carried out on isolated molecules and bulk crystal structures. For the isolated molecules, geometry optimizations of two-moiety – the phenyl ring and one EDOT – and three-moiety – the phenyl ring and two EDOTs – structures were completed at the ωB97XD/jun-cc-pvdz level of theory as implemented in the Gaussian 16 software suite.[41-43] All optimized, unconstrained geometries were confirmed as minima on the potential energy surface through normal mode analyses. Potential energy surfaces (PES), where select inter-moiety dihedral angles were held constant and the remainder of the molecules allowed to relax were also determined at the ωB97XD/jun-cc-pvdz level of theory. Atoms-in-molecules (AIM) analyses were carried out with topological analysis module in Multiwfn package.[44-45]

For calculations with periodic boundary conditions, DFT calculations were carried out with the Vienna Ab-initio Simulation Package (VASP),[46-47] making use of the Perdew, Burke, and Ernzerhof (PBE)[48] exchange-correlation functional based on experimentally solved structures. The electron-ion interactions were described with the projector augment wave (PAW) method.[48-49] The kinetic energy cutoff for the plane-wave basis set was set to 520 eV, and a Gaussian smearing with a width of 0.05 eV was employed.

To explore the disorder in the crystal structure of E-1F'-E, all possible configurations were generated by an iterative scheme and DFT relaxations were performed to identify the most stable configuration as described in the main-text. The convergence criterion of the total energy was set to 10^{-7} eV in the self-consistent loop and the force cutoff for relaxation was set to 10^{-2} eV/Å for cohesive energy calculations, or 10^{-4} eV/Å for extracting dihedral angles from the most stable configuration. The Brillouin-zone was sampled with a 3×3×2 Γ-centered grid.

ASSOCIATED CONTENT

Supporting Information. Experimental procedures for the synthesis of all new compounds. Data for absorption and emission spectroscopy, cyclic voltammetry, NMR data, DFT data. This material is available free of charge via the Internet at http://pubs.acs.org."

Cif files are available for compounds **1F** (CCDC 1914334), **2F** (CCDC 1914331) and **4F** (CCDC 1914332) from the Cambridge Crystallographic Database.

The data underpinning this submission are available to download from:
http://dx.doi.org/10.5525/gla.researchdata.818

AUTHOR INFORMATION

Corresponding Author

*peter.skabara@glasgow.ac.uk

Author Contributions

The manuscript was written through contributions of all authors. / All authors have given approval to the final version of the manuscript.

Funding Sources

Any funds used to support the research of the manuscript should be placed here (per journal style).
PIRSES-GA-2013-612670
NSF DMR-1627428

ACKNOWLEDGMENTS

TK, RP, RN and PJS thank the European Commission (Marie Curie Action of FP7, Grant No.: PIRSES-GA-2013-612670) for financial support.
The work at the University of Kentucky was supported by the National Science Foundation Designing Materials to Revolutionize and Engineer our Future (NSF DMREF) program under Award DMR-1627428. Supercomputing resources on the Lipscomb High Performance Computing Cluster were provided by the University of Kentucky Information Technology Department and Center for Computational Sciences (CCS).

REFERENCES

1. Jackson, N. E.; Savoie, B. M.; Kohlstedt, K. L.; Olvera de la Cruz, M.; Schatz, G. C.; Chen, L. X.; Ratner, M. A., Controlling Conformations of Conjugated Polymers and Small Molecules: The Role of Nonbonding Interactions. *J. Am. Chem. Soc.* **2013,** *135* (28), 10475-10483.
2. Conboy, G.; Spencer, H. J.; Angioni, E.; Kanibolotsky, A. L.; Findlay, N. J.; Coles, S. J.; Wilson, C.; Pitak, M. B.; Risko, C.; Coropceanu, V.; Bredas, J. L.; Skabara, P. J., To bend or not to bend - are heteroatom interactions within conjugated molecules effective in dictating conformation and planarity? *Mater. Horiz.* **2016,** *3* (4), 333-339.
3. Spencer, H. J.; Skabara, P. J.; Giles, M.; McCulloch, L.; Coles, S. J.; Hursthouse, M. B., The first direct experimental comparison between the hugely contrasting properties of PEDOT and the all-sulfur analogue PEDOT by analogy with well-defined EDTT-EDOT copolymers. *J. Mater. Chem.* **2005,** *15* (45), 4783-4792.

4. Eskandari, K.; Lesani, M., Does Fluorine Participate in Halogen Bonding? *Chem. Eur. J.* **2015,** *21* (12), 4739-4746.
5. Robertson, C. C.; Wright, J. S.; Carrington, E. J.; Perutz, R. N.; Hunter, C. A.; Brammer, L., Hydrogen bonding vs. halogen bonding: the solvent decides. *Chem. Sci.* **2017,** *8* (8), 5392-5398.
6. Skabara, P. J.; Arlin, J. B.; Geerts, Y. H., Close Encounters of the 3D Kind – Exploiting High Dimensionality in Molecular Semiconductors. *Adv. Mater.* **2013,** *25* (13), 1948-1954.
7. Thorley, K. J.; McCulloch, I., Why are S–F and S–O non-covalent interactions stabilising? *J. Mater. Chem. C* **2018,** *6* (45), 12413-12421.
8. Berridge, R.; Wright, S. P.; Skabara, P. J.; Dyer, A.; Steckler, T.; Argun, A. A.; Reynolds, J. R.; Ross, W. H.; Clegg, W., Electrochromic properties of a fast switching, dual colour polythiophene bearing non-planar dithiinoquinoxaline units. *J. Mater. Chem.* **2007,** *17* (3), 225-231.
9. Berridge, R.; Skabara, P. J.; Pozo-Gonzalo, C.; Kanibolotsky, A.; Lohr, J.; McDouall, J. J. W.; McInnes, E. J. L.; Wolowska, J.; Winder, C.; Sariciftci, N. S.; Harrington, R. W.; Clegg, W., Incorporation of fused tetrathiafulvalenes (TTFs) into polythiophene architectures: Varying the electroactive dominance of the TTF species in hybrid systems. *J. Phys. Chem. B* **2006,** *110* (7), 3140-3152.
10. Pozo-Gonzalo, C.; Khan, T.; McDouall, J. J. W.; Skabara, P. J.; Roberts, D. M.; Light, M. E.; Coles, S. J.; Hursthouse, M. B.; Neugebauer, H.; Cravino, A.; Sariciftci, N. S., Synthesis and electropolymerisation of 3 ',4 '-bis(alkylsulfanyl)terthiophenes and the significance of the fused dithiin ring in 2,5-dithienyl-3,4-ethylenedithiothiophene (DT-EDTT). *J. Mater. Chem.* **2002,** *12* (3), 500-510.
11. McEntee, G. J.; Skabara, P. J.; Vilela, F.; Tierney, S.; Samuel, I. D. W.; Gambino, S.; Coles, S. J.; Hursthouse, M. B.; Harrington, R. W.; Clegg, W., Synthesis and Electropolymerization of Hexadecyl Functionalized Bithiophene and Thieno 3,2-b thiophene End-Capped with EDOT and EDTT Units. *Chem. Mater.* **2010,** *22* (9), 3000-3008.
12. Zhao, W.; Li, S.; Yao, H.; Zhang, S.; Zhang, Y.; Yang, B.; Hou, J., Molecular Optimization Enables over 13% Efficiency in Organic Solar Cells. *J. Am. Chem. Soc.* **2017,** *139* (21), 7148-7151.
13. Zhang, Q.; Kelly, M. A.; Bauer, N.; You, W., The Curious Case of Fluorination of Conjugated Polymers for Solar Cells. *Acc. Chem. Res.* **2017,** *50* (9), 2401-2409.
14. Gao, J.; Wang, W.; Hu, Y.; Zhan, C.; Xiao, S.; Lu, X.; You, W., Transforming the molecular orientation of crystalline lamellae by the degree of multi-fluorination within D–A copolymers and its effect on photovoltaic performance. *J. Mater. Chem. C* **2018,** *6* (39), 10513-10523.
15. Asanuma, Y.; Mori, H.; Takahashi, R.; Nishihara, Y., Vinylene-bridged difluorobenzo[c][1,2,5]-thiadiazole (FBTzE): a new electron-deficient building block for high-performance semiconducting polymers in organic electronics. *J. Mater. Chem. C* **2019,** *7* (4), 905-916.
16. Crouch, D. J.; Skabara, P. J.; Heeney, M.; McCulloch, I.; Coles, S. J.; Hursthouse, M. B., Hexyl-substituted oligothiophenes with a central tetrafluorophenylene unit: crystal engineering of planar structures for p-type organic semiconductors. *Chem. Commun.* **2005,** (11), 1465-1467.
17. Crouch, D. J.; Skabara, P. J.; Lohr, J. E.; McDouall, J. J. W.; Heeney, M.; McCulloch, I.; Sparrowe, D.; Shkunov, M.; Coles, S. J.; Horton, P. N.; Hursthouse, M. B., Thiophene and selenophene copolymers incorporating fluorinated phenylene units in the main chain: Synthesis, characterization, and application in organic field-effect transistors. *Chem. Mater.* **2005,** *17* (26), 6567-6578.
18. Liu, Y.; Liu, Z.; Luo, H.; Xie, X.; Ai, L.; Ge, Z.; Yu, G.; Liu, Y., Benzothieno[2,3-b]thiophene semiconductors: synthesis, characterization and applications in organic field-effect transistors. *J. Mater. Chem. C* **2014,** *2* (41), 8804-8810.
19. Kim, H. G.; Kang, B.; Ko, H.; Lee, J.; Shin, J.; Cho, K., Synthetic Tailoring of Solid-State Order in Diketopyrrolopyrrole-Based Copolymers via Intramolecular Noncovalent Interactions. *Chem. Mater.* **2015,** *27* (3), 829-838.
20. Mueller, C. J.; Gann, E.; McNeill, C. R.; Thelakkat, M., Influence of fluorination in π-extended backbone polydiketopyrrolopyrroles on charge carrier mobility and depth-dependent molecular alignment. *J. Mater. Chem. C* **2015,** *3* (34), 8916-8925.
21. Zhang, W.; Shi, K.; Huang, J.; Gao, D.; Mao, Z.; Li, D.; Yu, G., Fluorodiphenylethene-Containing Donor–Acceptor Conjugated Copolymers with Noncovalent Conformational Locks for Efficient Polymer Field-Effect Transistors. *Macromolecules* **2016,** *49* (7), 2582-2591.
22. Lee, Y.-S.; Lee, J. Y.; Bang, S.-M.; Lim, B.; Lee, J.; Na, S.-I., A feasible random copolymer approach for high-efficiency polymeric photovoltaic cells. *J. Mater. Chem. A* **2016,** *4* (29), 11439-11445.
23. Weller, T.; Breunig, M.; Mueller, C. J.; Gann, E.; McNeill, C. R.; Thelakkat, M., Fluorination in thieno[3,4-c]pyrrole-4,6-dione copolymers leading to electron transport, high crystallinity and end-on alignment. *J. Mater. Chem. C* **2017,** *5* (30), 7527-7534.
24. Liu, J.; Ma, L.-K.; Li, Z.; Hu, H.; Ma, T.; Zhu, C.; Ade, H.; Yan, H., A random donor polymer based on an asymmetric building block to tune the morphology of non-fullerene organic solar cells. *J. Mater. Chem. A* **2017,** *5* (43), 22480-22488.
25. Wang, Y.; Tan, A. T.-R.; Mori, T.; Michinobu, T., Inversion of charge carrier polarity and boosting the mobility of organic semiconducting polymers based on benzobisthiadiazole derivatives by fluorination. *J. Mater. Chem. C* **2018,** *6* (14), 3593-3603.
26. Li, S.; Zhan, L.; Zhao, W.; Zhang, S.; Ali, B.; Fu, Z.; Lau, T.-K.; Lu, X.; Shi, M.; Li, C.-Z.; Hou, J.; Chen, H., Revealing the effects of molecular packing on the performances of polymer solar cells based on A–D–C–D–A type non-fullerene acceptors. *J. Mater. Chem. A* **2018,** *6* (25), 12132-12141.
27. Barłóg, M.; Kulai, I.; Ji, X.; Bhuvanesh, N.; Dey, S.; Sliwinski, E. P.; Bazzi, H. S.; Fang, L.; Al-Hashimi, M., Synthesis, characterization and crystal structures of novel fluorinated di(thiazolyl)benzene derivatives. *Organic Chemistry Frontiers* **2019,** *6* (6), 780-790.
28. Yum, S.; An, T. K.; Wang, X.; Lee, W.; Uddin, M. A.; Kim, Y. J.; Nguyen, T. L.; Xu, S.; Hwang, S.; Park, C. E.; Woo, H. Y., Benzotriazole-Containing Planar Conjugated

Polymers with Noncovalent Conformational Locks for Thermally Stable and Efficient Polymer Field-Effect Transistors. *Chem. Mater.* **2014,** *26* (6), 2147-2154.
29. Jo, J. W.; Jung, J. W.; Wang, H.-W.; Kim, P.; Russell, T. P.; Jo, W. H., Fluorination of Polythiophene Derivatives for High Performance Organic Photovoltaics. *Chem. Mater.* **2014,** *26* (14), 4214-4220.
30. Kim, M.; Park, W.-T.; Park, S. A.; Park, C. W.; Ryu, S. U.; Lee, D. H.; Noh, Y.-Y.; Park, T., Controlling Ambipolar Charge Transport in Isoindigo-Based Conjugated Polymers by Altering Fluorine Substitution Position for High-Performance Organic Field-Effect Transistors. *Adv. Funct. Mater.* **2019,** *29* (10), 1805994.
31. Huang, H.; Yang, L.; Facchetti, A.; Marks, T. J., Organic and Polymeric Semiconductors Enhanced by Noncovalent Conformational Locks. *Chem. Rev.* **2017,** *117* (15), 10291-10318.
32. Sotzing, G. A.; Reynolds, J. R.; Steel, P. J., Electrochromic Conducting Polymers via Electrochemical Polymerization of Bis(2-(3,4-ethylenedioxy)thienyl) Monomers. *Chem. Mater.* **1996,** *8* (4), 882-889.
33. Pepitone, M. F.; Eaiprasertsak, K.; Hardaker, S. S.; Gregory, R. V., Synthesis of bis[(3,4-ethylenedioxy)thien-2-yl]-substituted benzenes. *Tetrahedron Lett.* **2004,** *45* (29), 5637-5641.
34. Irvin, D. J.; Reynolds, J. R., Tuning the band gap of easily oxidized bis(2-thienyl)– and bis(2-(3,4-ethylenedioxythiophene))–phenylene polymers. *Polymers for Advanced Technologies* **1998,** *9* (4), 260-265.
35. Raimundo, J. M.; Blanchard, P.; Frere, P.; Mercier, N.; Ledoux-Rak, I.; Hierle, R.; Roncali, J., Push-pull chromophores based on 2,2 '-bi(3,4-ethylenedioxythiophene) (BEDOT) pi-conjugatiug spacer. *Tetrahedron Lett.* **2001,** *42* (8), 1507-1510.
36. Johnson, E. R.; Keinan, S.; Mori-Sánchez, P.; Contreras-García, J.; Cohen, A. J.; Yang, W., Revealing Noncovalent Interactions. *J. Am. Chem. Soc.* **2010,** *132* (18), 6498-6506.
37. Eskandari, K.; Zariny, H., Halogen bonding: A lump–hole interaction. *Chem. Phys. Lett.* **2010,** *492* (1), 9-13.
38. Pavan, M. S.; Durga Prasad, K.; Guru Row, T. N., Halogen bonding in fluorine: experimental charge density study on intermolecular F···F and F···S donor–acceptor contacts. *Chem. Commun.* **2013,** *49* (68), 7558-7560.
39. Xia, Y.; Viel, S.; Wang, Y.; Ziarelli, F.; Laurini, E.; Posocco, P.; Fermeglia, M.; Qu, F.; Pricl, S.; Peng, L., Rationalizing the F···S interaction discovered within a tetrafluorophenylazido-containing bola-phospholipid. *Chem. Commun.* **2012,** *48* (36), 4284-4286.
40. Mohan, N.; Suresh, C. H., A Molecular Electrostatic Potential Analysis of Hydrogen, Halogen, and Dihydrogen Bonds. *J. Phys. Chem. A* **2014,** *118* (9), 1697-1705.
41. Chai, J.-D.; Head-Gordon, M., Long-range corrected hybrid density functionals with damped atom–atom dispersion corrections. *Phys. Chem. Chem. Phys.* **2008,** *10* (44), 6615-6620.
42. Dunning Jr, T. H. J. T. J. o. c. p., Gaussian basis sets for use in correlated molecular calculations. I. The atoms boron through neon and hydrogen. **1989,** *90* (2), 1007-1023.
43. Frisch, M.; Trucks, G.; Schlegel, H.; Scuseria, G.; Robb, M.; Cheeseman, J.; Scalmani, G.; Barone, V.; Petersson, G.; Nakatsuji, H. J. R. A., Gaussian 16. **2016,** *3*.
44. Lu, T.; Chen, F., Quantitative analysis of molecular surface based on improved Marching Tetrahedra algorithm. *Journal of Molecular Graphics and Modelling* **2012,** *38*, 314-323.
45. Lu, T.; Chen, F., Multiwfn: A multifunctional wavefunction analyzer. *J. Comput. Chem.* **2012,** *33* (5), 580-592.
46. Kresse, G.; Furthmüller, J., Efficiency of ab-initio total energy calculations for metals and semiconductors using a plane-wave basis set. *Computational Materials Science* **1996,** *6* (1), 15-50.
47. Kresse, G.; Furthmüller, J., Efficient iterative schemes for ab initio total-energy calculations using a plane-wave basis set. *Phys. Rev. B* **1996,** *54* (16), 11169-11186.
48. Perdew, J. P.; Chevary, J. A.; Vosko, S. H.; Jackson, K. A.; Pederson, M. R.; Singh, D. J.; Fiolhais, C., Atoms, molecules, solids, and surfaces: Applications of the generalized gradient approximation for exchange and correlation. *Phys. Rev. B* **1992,** *46* (11), 6671-6687.
49. Kresse, G.; Joubert, D., From ultrasoft pseudopotentials to the projector augmented-wave method. *Phys. Rev. B* **1999,** *59* (3), 1758-1775.

Table of contents graphic

Non-covalent close contacts in fluorinated thiophene-phenylene-thiophene conjugated units: understanding the nature and dominance of O···H versus S···F and O···F interactions towards the control of polymer conformation